

Influence of Laser Marks on the Electrochemical Behaviour of the ASTM F139 Stainless Steel for Biomedical Application

*Eurico Felix Pieretti**, *Maurício David Martins das Neves*

Instituto de Pesquisas Energéticas e Nucleares (IPEN/CNEN), Av. Prof. Lineu Prestes 2242, Cidade Universitária, São Paulo – SP, 05422-970, Brazil

*E-mail: efpieretti@usp.br

Received: 1 February 2016 / *Accepted:* 5 March 2016 / *Published:* 1 April 2016

The aim of this work is to evaluate the effect of a laser marking technique on the microstructure and chemical composition at the surface of the ASTM F139 stainless steel and the influence of the surface modifications on its corrosion resistance. This is one of the most frequently used biomaterial for prosthesis manufacture. The laser effect on the corrosion resistance has been evaluated by electrochemical techniques, specifically electrochemical impedance spectroscopy. It was found that the laser marking reduces the corrosion resistance by modification of the microstructure and surface chemical composition affecting the surface passive layer, comparatively to the unmarked material. The surface and chemical composition was analyzed by scanning electron microscope coupled to a high-resolution field emission gun (SEM-FEG) and transmission electron microscopy (TEM) with microanalysis. TEM in areas affected by laser engraving showed a very high density of dislocations suggesting the presence of residual stresses induced by laser, decreasing the corrosion resistance of the stainless steel. Aluminum and silicon oxide inclusions were conveyed into the surface exposed to the corrosive electrolyte by melting the metallic matrix surrounding them during the incidence of the laser beam. The corrosive attack of this stainless steel matrix surrounding the oxide inclusions creates micro crevices, promoting pitting corrosion. This is the mechanism proposed to explain the increased susceptibility to localized corrosion associated to the areas affected by the laser marking process.

Keywords: Biomedical engineering, biointerfaces, laser engraving, electrochemistry.

1. INTRODUCTION

The ASTM F139 stainless steel is one of the metallic biomaterials most used for implants fabrication due to its mechanical and corrosion properties, and mainly its comparatively low cost. Stainless steel implantable medical devices are also used as permanent or short-term implants to help bone healing.

The implants, prior to use, undergo a marking process before being sterilized whose function is to provide a clear identification and traceability in order to correlate the end condition to its fabrication process. One of the methods used for marking implants is the laser process. This process involves melting the area by a laser beam and this strongly affects the material and might affect its corrosion resistance. The implantable medical devices used in mobile joints of the human body, as well as for dental purposes require biocompatibility with the surrounding tissues and organs, mechanical strength and corrosion resistance.

The marking technique is commonly used for recognition and classification or traceability of implants enabling a posterior analysis of the metallic implantable medical device after its use. This process strongly affects the characteristics of the surface exposed to the corrosive human body fluids, such as microstructure, composition and surface roughness.

The body fluids constitute a hostile environment for the implant leading to corrosion of implants. Corrosion might also be associated with friction/wear and this might lead to metallic particles detachment. Metallic particles released into the body fluids due to the corrosion process may move passively, through tissue and/or circulatory system or might be actively transported [1], affecting organs which are away from the biomaterial and might also compromise the biocompatibility of the biomaterial. It was found that during friction the current densities were higher than those under stationary conditions. It was also observed a range of floating current density caused by the formation and breaking of the passive film. As expected, it was also found that the more stable is the passive film, the lower the amount of released metal ions from the surface [2].

According to Anderson [3], a biocompatible biomaterial for a given use is not necessarily biocompatible to another area of application. In order to facilitate the selection of a suitable material for implantation, the nature of the contact between the biomaterial and the body region and the duration of the contact should be considered.

The corrosion resistance of a biomaterial is strongly influenced by its microstructure, chemical composition, roughness and design. [4]. The corrosion resistance of the metallic implants depends on the protective properties of the passivating oxide layer which is formed by the interaction of the surface with the surrounding environment [4-6]. Although the thickness of the oxide layer is only a few nanometers, it acts as a semiconducting layer between the metallic surface and the biologic system.

Localized corrosion in stainless steels usually starts at specific sites at the surface which are related to heterogeneities, such as inclusions [5, 7-8]. At these sites, passivity breakdown occurs and, under certain circumstances, leads to rapid and localized dissolution.

Qi *et al.* [10] studied the marking process of stainless steels by means of laser beams. They used a laser type Q-switched Nd: YAG and evaluated the influence of pulse frequency, energy and speed on the quality of marking produced. Qualitatively comparing the depth, width and contrast generated by the marking, it was observed that the pulse frequency was the parameter that most affected oxidation, and consequently, the contrast of the engravings.

Similarly, Leone *et al.* [11] found that it is the pulse rate parameter that most interfered with the contrast obtained in the digital images of the surfaces subjected to a marking process. In their study they used the same kind of laser and the same parameters adopted by Qi *et al.* in their work [10], to

mark an AISI 304 SS. They found that surface roughness and oxidation of the engraved surface increased with the pulse frequency.

The effect of the surface roughness on the corrosion resistance of the stainless steel has been investigated in the literature. Hong and Nagumo [12] published a research elucidating the effect of surface roughness in the early stages of pitting corrosion of the AISI 301 stainless steel in a solution of 0.5 M NaCl. The results were presented as impedance diagrams and polarization curves. The research concluded that the coefficient of Warburg impedance diminishes as the surface smoothness increases. They related these results to the number of metastable pits found in a smoother surface which are fewer than that found in rougher surfaces.

Patrikar [13] conducted a research to model and simulate surface roughness using numerical methods and the use of neural networks. He stated that surface roughness causes significant effects on the electrical properties of materials, such as capacitance, electronic conductivity, and peaks in the electric field, among others. Besides, generic electrical resistance in a thin metal film increases due to electron scattering, point defects, impurities and grain orientation, once the electrical resistance of thin films increases with the surface roughness.

In the present study, the effects of the laser marking process on the ASTM F139 stainless steel microstructure and pitting corrosion resistance have been investigated.

2. EXPERIMENTAL

ASTM F139 stainless steel samples, with the following composition (wt. %): 0.38 Si, 2.09 Mn, 0.026 P, 2.59 Mo, 18.32 Cr, 14.33 Ni, 0.023 C, 0.0003 S, and Fe balance, were marked by pulsed Nd:YAG laser. The marking technique consisted of recording a sequence of numerical symbols on the surface in order to cover the largest area of the samples.

The corrosion resistance was evaluated by electrochemical impedance spectroscopy (EIS). The electrochemical tests were carried out using a Gamry PCI4/300, with a flat-cell of three electrodes composed of a working electrode with 1.0 cm² exposed area, a counter-electrode of platinized platinum and Ag/AgCl (3M) reference electrode. The electrolyte used consisted of a naturally aerated phosphate buffer solution (PBS), at 37°C, with the following composition: NaCl 8.0 g/L, KCl 0.2 g/L, Na₂HPO₄ 1.15 g/L, KH₂PO₄ 0.2 g/L, with a pH of 7.4, and a conductivity of 15.35 mS. Electrochemical impedance spectroscopy tests of marked and unmarked samples were carried out after 17 h of samples immersion in the electrolyte.

Surface analyses were conducted using a scanning electron microscope coupled to a high-resolution field emission gun (SEM-FEG, FEI - INSPECT F50), and a transmission electron microscope with microanalysis (TEM-EDX) JEOL, model JSM-2100. For TEM analyses, the samples were cut in the form of very thin sheets and then electrolytically refined and cut into circular shape.

3. RESULTS AND DISCUSSION

The corrosion resistance of the ASTM F139 stainless steel marked by laser was evaluated by electrochemical impedance spectroscopy analyzing an area corresponding to 1 cm² and samples without marks were also evaluated for comparison reasons.

Figure 1 shows the Nyquist diagrams for the two types of tested surfaces. Lower impedances were associated to the laser marked surfaces indicating a deleterious effect of the engraving technique on the material corrosion resistance. Equivalent electric circuits (EEC) were proposed and adjusted to the EIS data. Two equivalent electric circuits (EEC) were proposed, depending on the type of surface tested [14] and these are showed in Figure 2.

The EEC models proposed to simulate the experimental results took into consideration the electrochemical behavior, that is, the charge transfer processes at two interfaces, oxide film-electrolyte and metallic substrate-oxide film. These have been largely used in the literature to simulate the electrochemical behavior of passive stainless steels [14-18]. In the EEC proposed in this study, CPE is a constant phase element, C is an ideal capacitor and R represents the resistance at the interfaces. The R_1/CPE_1 pair was associated to the oxide film-electrolyte interface, whereas the R_2/C_2 pair was related to the substrate-oxide film interface. The values obtained for the EEC components are shown in Table 1. Lower R_1 values were associated to the laser marked samples comparatively to the unmarked ones. This resistance indicates that cation release at the oxide film/electrolyte interface was eased in the laser marked material, suggesting that the passive film on the laser marked areas is less stable than that on the unmarked ones. Consequently, the generation of n-type defects is increased and also that of the p-type defects in order to maintain charge neutrality inside the passive film. The n_1 values for the laser marked areas indicated a more heterogeneous surface than the unmarked ones, as expected. It is worth to emphasize that n indicates the surface heterogeneity. The higher CPE_1 values associated to the laser marked areas comparatively to the unmarked ones, support the indication of a more reactive surface for the first type.

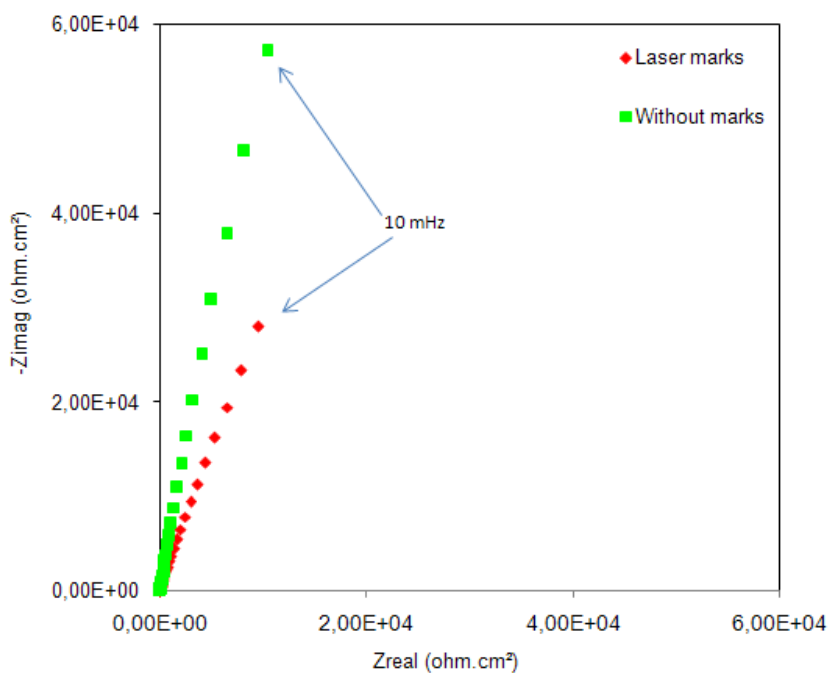


Figure 1. Nyquist diagrams for ASTM F139 stainless steel samples either without marks or with laser marks at the surface.

It must be pointed out that the resistance related to the charge transfer processes at the metallic substrate-oxide film interface (R_2) is of the order of 10^4 times higher comparatively to that associated to the oxide layer-electrolyte interface and, consequently, it is the main responsible for the corrosion resistance of the passive film. The value of R_2 associated to the unmarked surfaces is one order of magnitude higher comparatively to the laser marked surface. The higher generation of defects at the metallic substrate-oxide film interface for the laser marked surface might have been caused by the high deformation introduced during the too rapid melting and solidification process occurring at the laser affected sites affecting the properties of the oxide layer formed. This can be seen in the micrograph of Figure 3, obtained by scanning electron microscopy (SEM) that shows the area of the surface affected by the laser beam.

The EIS results showed that the laser marking treatment had a deleterious effect on the corrosion resistance of the ASTM F139 SS, decreasing the resistance of the oxide film formed at the surface.

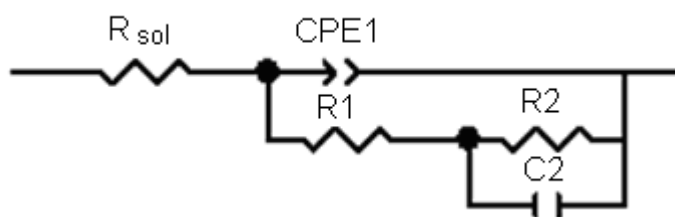


Figure 2. Equivalent electrical circuit proposed to adjust the experimental data obtained for the ASTM F139 stainless steel samples, either without marks or with laser marks.

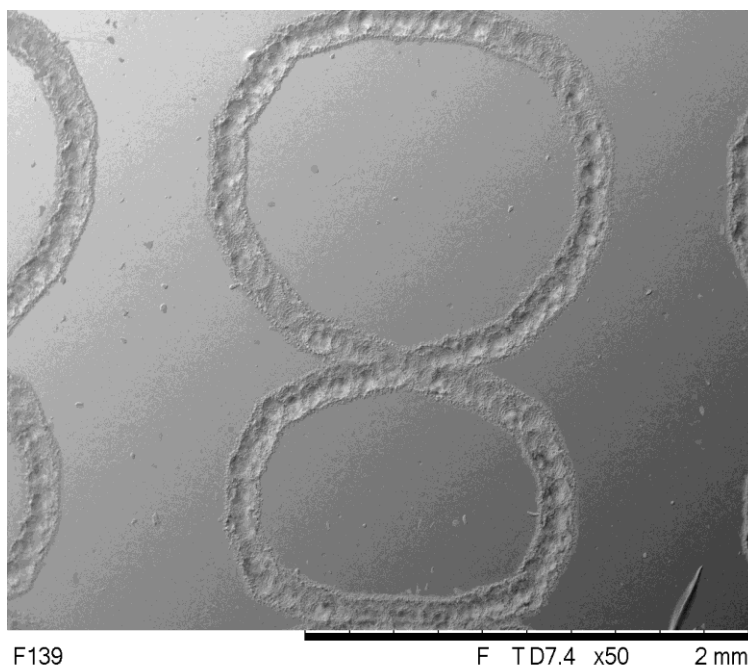
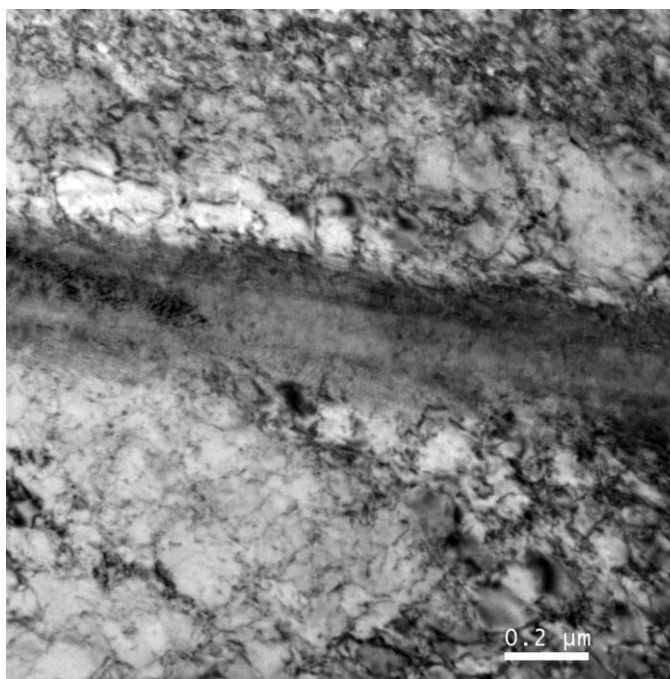


Figure 3. SEM micrograph of the ASTM F139 stainless steel surface with laser marked areas.

Table 1. Values obtained from fitting the experimental data to the equivalent electrical circuit model proposed and shown in Figure 2.

Type of material	R_{sol} (Ωcm^2)	CPE_1 ($\text{cm}^{-2}\text{s}^{-n}\Omega^{-1}$)	n_1	R_1 (Ωcm^2)	C_2 ($\text{cm}^{-2}\text{s}^{-n}\Omega^{-1}$)	R_2 (Ωcm^2)
Without marks	28.6	20.7×10^{-6}	0.927	329.5	2.20×10^{-6}	1.82×10^6
Laser marked	25.6	45.6×10^{-6}	0.822	72.0	1.64×10^{-6}	3.60×10^5

Figure 4 displays images obtained by transmission electron microscopy (TEM) of areas of the ASTM F139 SS microstructure which have been affected by laser engraving. The introduction of a large concentration of defects in the material by the laser marking process is indicated in Figure 4. A very high density of dislocations is indicated by the large number of lines showed and this suggests the presence of residual stresses induced in the surface by the laser mark. The deformation bands with high dislocations density are considered as regions of high stress decreasing the localized corrosion resistance [19].

**Figure 4.** Transmission Electron Microscopy (TEM) of the laser engraved ASTM F 139 SS, showing high dislocation density and the morphology of a stripe surrounded by a highly deformed material.

EDX semiquantitative analyses performed at stripe line seen in Figure 4 showed that these are rich in chromium, but also in silicon and aluminum, as Figure 5 (a) shows. This is supported by EDX spectrum obtained at the matrix away from the inclusions as indicated in Figure 5 (b).

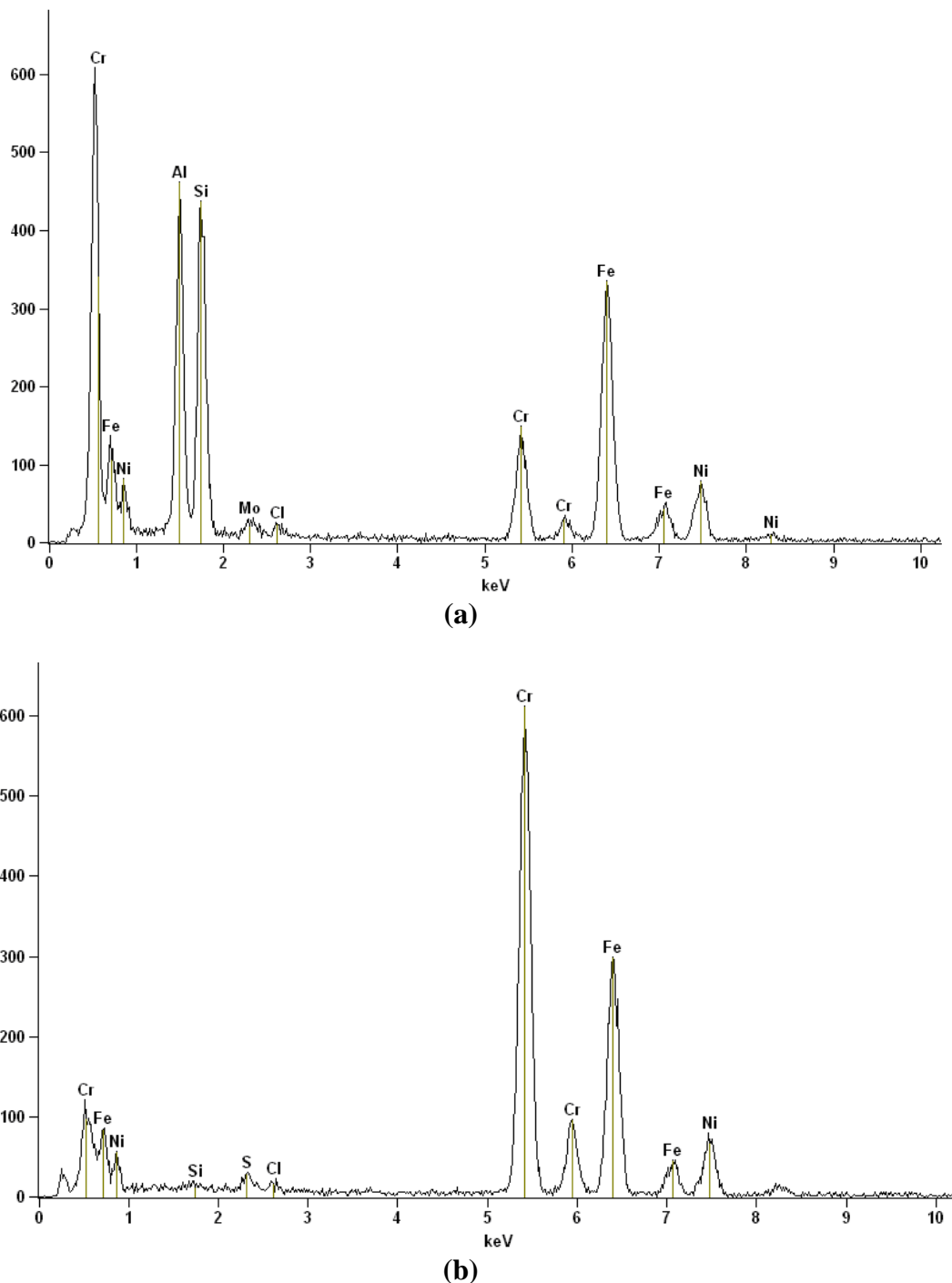


Figure 5. (a) EDX semiquantitative spectrum of ASTM F139 SS marked by laser, performed at the stripe line shown in Fig. 4, presenting chromium, aluminum and silicon peaks, (b) area of the matrix away from the line.

EDX semiquantitative analyses indicated the presence of non-metallic inclusions containing aluminum, silicon, calcium, but also evidenced traces of chlorine and sodium from the saline (PBS) solution used in electrochemical tests. Pitting starts due to the adsorption of aggressive species, mainly chloride ions from the solution, at the oxide surface followed by film breakdown at the weakest places of the passive film. Consequently, it is expected to find chloride associated to the pits [20].

The results show that the chemical composition at adjacent sites showed great variation at the laser marked areas.

Dowling *et al.* [21] evaluated the corrosion resistance of the UNS S44400 ferritic stainless steel in a solution of 3.5% NaCl at 35 °C. The results showed that pitting corrosion was closely related to the type, quantity, and size of intermetallic inclusions present in the material. They conducted cyclic polarization tests with polished samples to identify the nucleation of pits in the ferritic stainless steel, interrupting the test soon after the current started increasing due to breakdown of the passive film. It was found that chromium oxide inclusions, alumina inclusions and complex inclusions of manganese sulfide and silicon dioxide led to crevice corrosion between the inclusions and the matrix.

A similar mechanism has been found for austenitic stainless steel with laser markings, where the sites of pits nucleation were investigated by accomplishing polarization tests. By analyzing the polarized surface by SEM-FEG, it was found that the inclusions had originated areas of micro or nano cracks between them and the matrix material [14].

Figure 6 shows a micro-pit at the laser marked areas surrounding a significant amount of non-metallic inclusions.

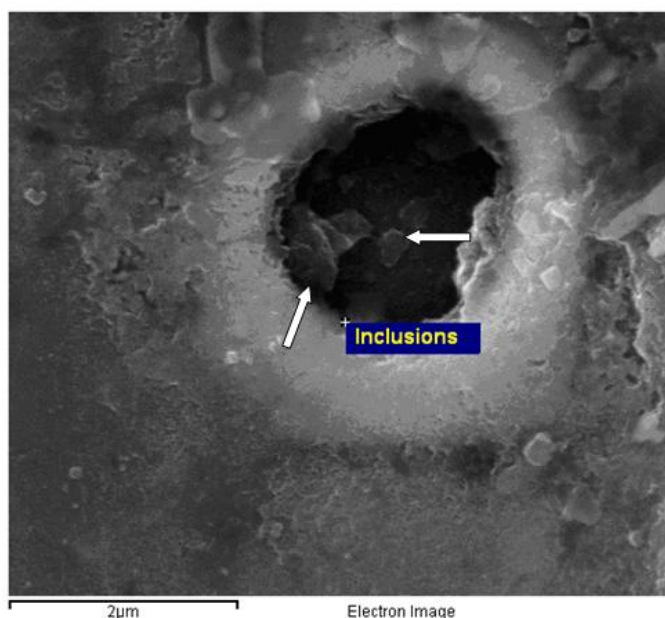


Figure 6. SEM-FEG image of a pit in the early stages of formation indicating the presence of non metallic inclusions inside.

Lower pitting resistance for laser marked surface could also be explained by the thermal effect of the laser marking process towards the roughness of the stainless steel [18]. This reduces the breakdown potential of the passive film. The laser marking occurs by melting the surface to produce the desired image, in this case, resulting in rough surface finishing. According to Hong and Nagumo [12], smoother surfaces reduce the incidence of homogeneous metastable pits mainly by reducing the number of sites capable of being activated in the growth of metastable pits.

Considering the deleterious effect of laser marking on the corrosion resistance of the stainless steel studied, it is proposed that the areas most affected by the laser beam are likely the most susceptible to pitting initiation. This effect was observed in recent studies, even in protein-based medium [22-24]. The heating effect creates a high concentration of defective sites at the passive film, besides producing a rough surface finish. The attack of the weakest areas of the passive film exposes the metallic substrate and generates micro crevices that lead to differential aeration cells and, consequently, promotes propagation of the initiated pits.

4. CONCLUSIONS

The results of the present study showed that the laser engraving technique used for biomaterials traceability induces large variation in the microstructure and the chemical composition of the surface. Besides, it induces a high concentration of defects and increases roughness. The inclusions found at the surface were composed mainly oxides or mixed oxides which are ceramic type of inclusions which are not melted by the fast incidence of the laser beam, remaining at the surface. The formation of a new chromium free phase was also detected by diffraction analysis coupled to transmission electron microscopy. These modifications in the material microstructure led to decrease the corrosion resistance, mainly the pitting resistance.

ACKNOWLEDGEMENTS

The authors acknowledge CNPq for the financial support, under grant number Process: 350798/2014-1, Project: 459565/2013-3; the Instituto de Ortopedia e Traumatologia of the Hospital das Clínicas da Faculdade de Medicina da Universidade de São Paulo and Dr. I. Costa, PhD.

References

1. J. Black, *Biomaterials* 5 (1984) 11.
2. Y. Okasaki, *Biomaterials* 23 (2002) 2071.
3. J. M. Anderson, *Mater. Research* 31 (2001) 81.
4. S. Virtanen, I. Milošev, E. Gomez-Barrena, R. Trebše, J. Salo, Y. T. Kontinen, *Acta Biomaterialia* 4 (2008) 468.
5. C. Punckt, M. Bölscher, H. Rotermund, A.S. Mikhailov, L. Organ, N. Budianky, J.R. Scully, J.L. Hudson, *Science* 305 (2004) 1133.
6. X. Cheng, X. Li, C. Dong, *Int. J. Minerals, Metallurgy and Materials* 16 (2009) 170.
7. C. C. Shih, C. M. Shih, Y. Y. Su, L. H. J. Su, M. S. Chang, S. J. Lin, *Corros. Sci.* 46 (2004) 427.
8. A. Shahryari, S. Omanovic, J. A. Szpunar, *Mater. Sci. and Eng. C* 28 (2008) 94.
9. M. Pourbaix, L. Klimzack-Mathieiu, C. Merterns, J. Meunier, C. Vanluegen-Haghe, L. de Munck, J. Laureys, L. Neelemans, M. Warzee, *Corros. Sci.* 3 (1963) 239.
10. J. Qi, K. L. Wang, Y. M. Zhu, *J. Mater. Proces. Tech.* 139 (2003) 273.
11. C. Leone, S. Genna, G. Caprino, I. De Iorio, *J. Mater. Proces. Tech.* 210 (2010) 1293.
12. T. Hong, M. Nagumo, *Corros. Sci.* 39 (1997) 1665.
13. R. M. Patrikar, *Ap. Surf. Sci.* 228 (2004) 213.
14. E. F. Pieretti, I. Costa, *Electrochim. Acta*, 114 (2013) 838.

15. N. E. Hakiki, M. F. Montemor, M. G. S. Ferreira, M. Da Cunha Belo, *Corros. Sci.* 42 (2000), 687.
16. M. Da Cunha Belo, N. E. Hakiki, M. G. S. Ferreira, *Electrochim. Acta* 44 (1999) 2473.
17. P. Schmuki, H. Böhni, J. A. Bardwell, *J. Electrochem. Soc.* 142 (1995), 1705.
18. E. F. Pieretti, E. J. Pessine, O. V. Correa, W. de Rossi, M. D. M. das Neves, *Int. J. Electrochem. Sci.*, 10 (2015) 1221.
19. U. Kamachi Mudali, P. Shankar, S. Ningshen, R. K. Dayal, H. S. Khatak, B. Raj, *Corros. Sci.* 44 (2002) 2183.
20. H. Asteman, J. E. Svensson, L. G. Johansson, *Oxidation of Metals* 57 (2002) 193.
21. N. J. E. Dowling, Y. H. Kim, S. K. Ahn, Y. D. Lee, *Corrosion* 55 (1999) 187.
22. E. F. Pieretti, S. M. Manhabosco, L. F. P. Dick, S. Hinder, I. Costa, *Electrochim. Acta*, 124 (2014) 150.
23. E. F. Pieretti, R. P. Palatnic, T. P. Leivas, I. Costa, M. D. M. das Neves, *Int. J. Electrochem. Sci.*, 9 (2014) 2435.
24. E. F. Pieretti, I. Costa, R. A. Marques, T. P. Leivas, M. D. M. das Neves, *Int. J. Electrochem. Sci.*, 9 (2014) 3828.

© 2016 The Authors. Published by ESG (www.electrochemsci.org). This article is an open access article distributed under the terms and conditions of the Creative Commons Attribution license (<http://creativecommons.org/licenses/by/4.0/>).